Penerbit Akademia Baru

CFD Letters

Journal homepage: www.akademiabaru.com/cfdl.html
ISSN: 2180-1363

Computational Methods for Predicting A Pico-Hydro Cross-Flow Turbine Performance

Open Access

Warjito[1], Budiarso[1], Celine Kevin[1,*], Dendy Adanta[1], Aji Putro Prakoso[1]

[1] Department of Mechanical Engineering, Faculty of Engineering, Universitas Indonesia, Indonesia

ARTICLE INFO

Article history:
Received 20 October 2019
Received in revised form 15 December 2019
Accepted 20 December 2019
Available online 28 December 2019

ABSTRACT

Usually, to find out the maximum performance of a turbine, an experimental test is carried out using the loading (preload) variations method. The high proportion of torque (τ) and runner rotation velocity (U) is an indication of maximum turbine performance. However, if there is mistaken in the shape of geometry it takes more time and funds. The correct solution is a prediction using the computational fluid dynamics (CFD) method. This study proposes the method to predict the maximum conditions of pico-hydro cross-flow turbines by comparing the preload acting on runners by CFD method. So, if something goes wrong in the design can be corrected immediately. The preloads variation in this study consists of 0 N·m, 30 N·m, 45 N·m, and 60 N·m with the head condition of 1 meter and mass flow of 10.5 kg/s. The CFD method with six-degree of freedom (6-DoF) was selected because the rotational turbine is one of the computational results not as boundary conditions. The turbulence model k-ε standard has been used to predict the turbulent flow. Based on results, transient data (torque and runner rotational velocity) obtained from computing is similar to testing, which fluctuates and becomes steady. Furthermore, the used 45 N·m preload has more stable and had higher efficiency than the other. The turbine with 45 N·m preload produced 60.07% efficiency. This indicates that the turbine that is designed will work optimally at 45 N·m preload. Thus, CFD method with 6-DoF feature proposed to predict a pico-hydro cross-flow turbine performance can be an alternative before the turbine is manufactured to be tested or implemented.

Keywords:
Computational; pico-hydro; cross-flow turbine; 6-DoF; preload

1. Introduction

An estimated that 14% of the world population does not have access to electricity which is mostly in the developing country [1]. About 84% of those who do not have access to electricity are in rural areas and more than 95% of those are in developing countries [1]. The matter of energy resources is one of the problems faced in the procurement of electricity. Hence, the use of renewable energy is the solution to this problem [2]. There is a wide variety of renewable energy such as hydro, wind, solar, and other natural forces. Today, the most widely used renewable energy is hydropower [2].

* *Corresponding author.*
E-mail address: celinekevin.ck@gmail.com (Celine Kevin)

Pico hydro is a hydropower plant that generates electricity under 5 kW [3]. This scale is suitable for the small-rural area that requires only a small amount of electricity daily. Compared to fossil fuel power plant, the pico-hydro gives us a low-cost electricity generation with the least pollution [4].

A pico-hydro cross-flow turbine is suitable to use in remote areas because of stable efficiency with a high deviation of discharge conditions, simple shape, and low investment cost compared to other types [5]. Subsequently, the cross-flow turbine has another advantage, such as less maintenance requirement, long life span, simple or less infrastructure, and economically friendly [6]. Thus, the selection of a cross-flow turbine for electrification in rural areas is considered appropriate because it has a simple design, modest efficiency, and it does not require high-head [7].

Cross-flow turbines are turbines that are used to convert kinetic energy of water to mechanical energy to rotate a shaft [4]. In contrast to other types of turbines, cross-flow turbines do not have radial or axial flow. In cross-flow turbines, the flow of water will cross the turbine blades.

To maximize the performance of cross-flow turbines, several methods can be used such as analytical, computational, and experimental methods. Many experts have selected the computational fluid dynamics (CFD) method because it can represent a turbine's flow pattern in more detail than other methods [8]. To get the precision of predictions using the CFD method, the model was used must similar to the real conditions [9]. In order for the model to be similar against real conditions, the density of material (moment of inertia) and load (preload) of the runner should be the boundary conditions of the simulation. However, there has been no attention that discusses the moment of inertia and preload in the simulation of a pico-hydro cross-flow turbine. This study will focus on reviewing preload.

Preload is a load received by the runner to find out the maximum performance of a turbine. The greater the load, the greater the torque (τ) needed to turn the runner or generator. Usually, preload or loading is only done by experiment. Using the CFD method, this study will propose methods to predict the maximum conditions of pico-hydro crossflow turbines by comparing the preload acting on runners. The CFD method was chosen because if something goes wrong in the design it can be corrected immediately.

2. Methodology

A solid-3D model was created in computer-aided design (CAD) software according to the available designs. The specific design parameters are shown in Table 1. Figure 1 shows the 3D model of the cross-flow turbine.

Table 1
Design Parameters

Design Parameter	Value
Number of blades, z	20
Outer diameter, D_o	180 mm
Inner diameter, D_i	117 mm
Blade's length, L	142 mm
The angle of attack, α	22°
Blade's inlet angle, β	42 °

The computational method was obtained by using ANSYS® FLUENT 18.1™. In this study, a 2D transient domain was used to perform the simulation. The 2D domain was created in Ansys Design Modeler, with the thin surface feature. Multiphase model volume with implicit volume fraction parameters and body force equation was selected based on the condition that has the water phase and air phase. The standard k-ε turbulent model also used in this simulation because it has a high accuracy of backflow and rotation in simulation [10]. The standard k-ε turbulent model was chosen because based on its y^+ value, it is on the k-ε turbulent model y^+ range. As for the k-ε turbulent model, the y^+ range is 30 to 300 [11]. The average y^+ value at blade obtained in this study is 40.51. The simulation also uses a dynamic mesh setting with six degrees of freedom (6-DOF) user-defined function. The 6-DOF was chosen because it can represent the fluid dynamics and physics phenomenon on the cross-flow turbine impeller [12]. The equations are discretized using second-order upwind interpolation schemes in selected CFD packages and SIMPLE algorithms. The SIMPLE method was chosen because it uses relationship between velocity and pressure corrections to enforce mass conservation and to obtain the pressure field [13]. The second-order upwind discrete scheme was used to satisfy the requirements for precision and steady-state [10]. The governing equations for k-ε are available in Eq. (1) for k and (2) for ε [13]

$$\frac{\partial}{\partial t}(\rho k) + \frac{\partial}{\partial x_i}(\rho k u_i) = \frac{\partial}{\partial x_j}\left[\left(\mu + \frac{\mu t}{\sigma k}\right)\frac{\partial k}{\partial x_j}\right] + Gk + Gb - \rho\varepsilon - Y_M + S_K \quad (1)$$

$$\frac{\partial}{\partial t}(\rho \varepsilon) + \frac{\partial}{\partial x_i}(\rho \varepsilon u_i) = \frac{\partial}{\partial x_j}\left[\left(\mu + \frac{\mu t}{\sigma \varepsilon}\right)\frac{\partial \varepsilon}{\partial x_j}\right] + C_{1\varepsilon}\frac{\varepsilon}{k}(G_k + C_{3\varepsilon}G_b) - C_{2\varepsilon}\rho\frac{\varepsilon^2}{k} + S_\varepsilon \quad (2)$$

where,

Gk = generation of turbulence kinetic energy due to the mean velocity gradient
Gb = generation of turbulence kinetic energy due to buoyancy
Y_M = contribution of the fluctuating dilatation incompressible turbulence to the overall dissipation rate
$C_{1\varepsilon}$, $C_{2\varepsilon}$, and $C_{3\varepsilon}$ = constants
∂k and $\partial\varepsilon$ = turbulent Prandtl number for k and ε
S_K and S_ε = user-defined source terms

In this simulation, the main fluid used was water. So, in the inlet, the water volume fraction (α_w) value was 0 and the air volume fraction (α_a) value was 1, which means there was no water in the inlet in the initial condition. The phasic volume fraction relies on the premise that the volume fractions are a continuous function in the spatial and temporal domain and the total sum of the volume fraction of all phases is one [14]. This simulation is carried out using a pressure inlet and pressure outlet as the boundary condition. The pressure inlet boundary condition was chosen because, in a cross-flow turbine, the inlet is converting pressure to velocity [5]. The pressure at the inlet is set at 9810 Pa with the operating pressure based on the head height of 1 m. Simulations were carried out 4 times, with variations of preload of 0 N.m, 30 N.m, 45 N.m, and 60 N.m.

A mesh independence study was executed using the single-phase – steady method. Mesh is an area where calculations will be made. Generally, the number of mesh is described as the number of elements. On the mesh independency test, variations in the number of mesh were used, namely 37589, 66079, 122408, and 230162 elements. The numbers of mesh were chosen to get a ratio value of 2.

In the mesh independency test, it can be seen that the larger the number of mesh, the smaller the torque deviation produced. Using the Richardson extrapolation method [15], the estimated exact value of torque is 84.44925382 N.m. It can be concluded that the number of mesh 122408 (84.5082 N.m) has the least torque error (0.0698%) value compared to the other number of mesh variations.

Thus, the number of mesh 122408 is good enough to use for the simulation. Figure 2 shows the mesh visualization with a 122408 number of elements. Table 2 shows the mesh independency test result.

Fig. 1. 3D model of the cross-flow turbine

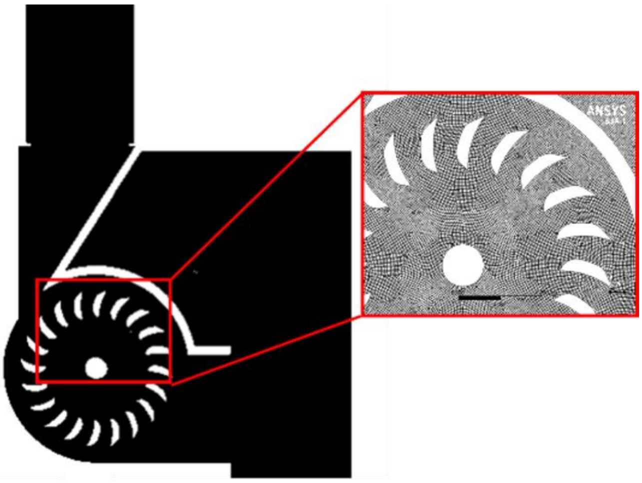

Fig. 2. 2D Domain mesh visualization – 122408 elements

Table 2
Mesh Independency Test Result

Number of Elements	Torque, τ	Grid Refinement Ratio	Grid Convergence Index
37589	93.17 N·m	6	-
66079	84.94 N·m	4	2.224 %
122408	84.51 N·m	2	0.094 %
230162	84.45 N·m	1	0.012 %
~	84.45 N·m	0	-

Each simulation will run for 5 s. The number of timesteps is 5000 timesteps with timestep size of 0.001 and 150 iterations for each timestep. The timestep size was chosen based on the timestep independency study. In the timestep independency test, it can be seen that the number of timestep 0.001 has the smaller the torque deviation produced. Using the Richardson extrapolation method [15], the estimated exact value of torque is 0.990 N·m. It can be concluded that the timestep size of 0.001 (0.988 N·m) has the least torque error (0.20%) value compared to the other timestep size variations. Thus, the timestep size of 0.001 s is good enough to use for the simulation. Table 3 shows the timestep independency test results.

Table 3
Timestep Independency Test Result

Timestep size	Torque, τ	Normalized Grid Spacing	Timestep Convergence Index
0.002	0.986 N·m	2	0.086
0.001	0.988 N·m	1.41	0.028
0.0005	0.987 N·m	1	0.035
~	0.990 N·m	0	-

3. Results

From Figure 3, shows that the torque (τ) produced is inversely proportional to the runner's rotation velocity (U). Furthermore, the greater the preload gave, the resulting torque (τ) increases but fluctuates, while the resulting U decreases but more stable. These results are similar to

Penerbit Akademia Baru

experimental results where there are transient and stable data. Based on Figure 3(a) and 3(b), the stable data occur in timestep 3750 and above, at this time the data obtained can be processed. Table 4 is the data that has been processed.

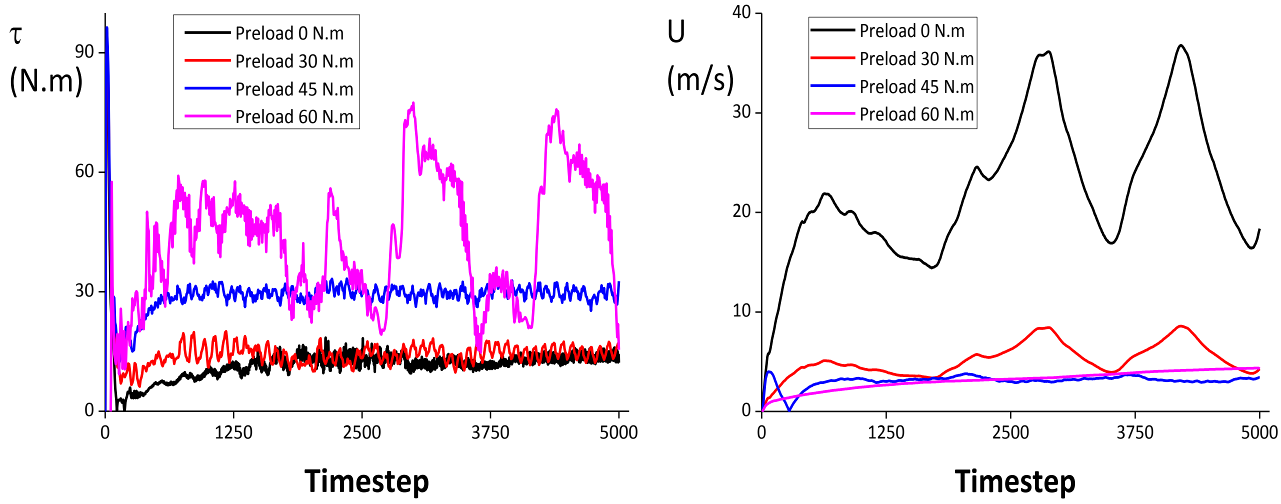

a) τ simulation results

b) U simulations results

Fig. 3. The computational results

Table 4 shows that with the head condition of 1 m, the efficiency of a cross-flow turbine with preload 45 N.m produced a higher efficiency than others. This is expected at 45 N.m preload, the resulting τ and U is more stable than the others. Furthermore, this shows that the maximum condition of the designed crossflow turbine is at 45 N.m preload with a U/W ratio of 0.75. In real conditions, the efficiency of impulse turbine (crossflow, Turgo and Pelton turbine) occurs at U/W of 0.5 [16]. The computation results obtained do not take into account losses due to friction so that the optimum U/W ratio will be obtained at 0.5 (if tested in real conditions).

Table 4
Computational results with variations in preload

Parameter	Preload			
	0 N·m	30 N·m	45 N·m	60 N·m
U/W	0.99	0.95	0.75	0.35
Wheel velocity stable, U	4.26 m/s	4.10 m/s	3.21 m/s	1.51 m/s
Average Torque, τ	1.51 N·m	14.77 N·m	29.73 N·m	44.89 N·m
Efficiency, η	6.39 %	19.29 %	60.07 %	7.47 %

Pressure contour and streamline are used to analyse whether the simulation results are similar to real conditions (qualitative analysis). In some cases of CFD, verification and validation of CFD results using qualitative methods are important because even though the setup is correct, but the physical phenomenon is not in accordance with applicable law, the results obtained are not unjustified. The water volume fraction and streamline are shown only in the water phase.

The pressure contour can be seen in figure 4. At each difference in preload loading, it can be seen that pressure has a large value when the fluid first collides with the blade tip. When the preload is given 0 N.m, the turbine will spin very fast which causes the water not to pound the blade. The wheel spin very fast thought to be the cause of the low torque produced. The high-velocity area can be seen on the pressure contour where the pressure is low (at the blade area). Compared to when the turbine was given a preload of 45 N.m, the water pounded almost on all blades. This happens because the given preload acts like a brake which slows the turbine's rotation so that the water can hit the blade. With a large number of blades pounded by water, then the power produced will increase.

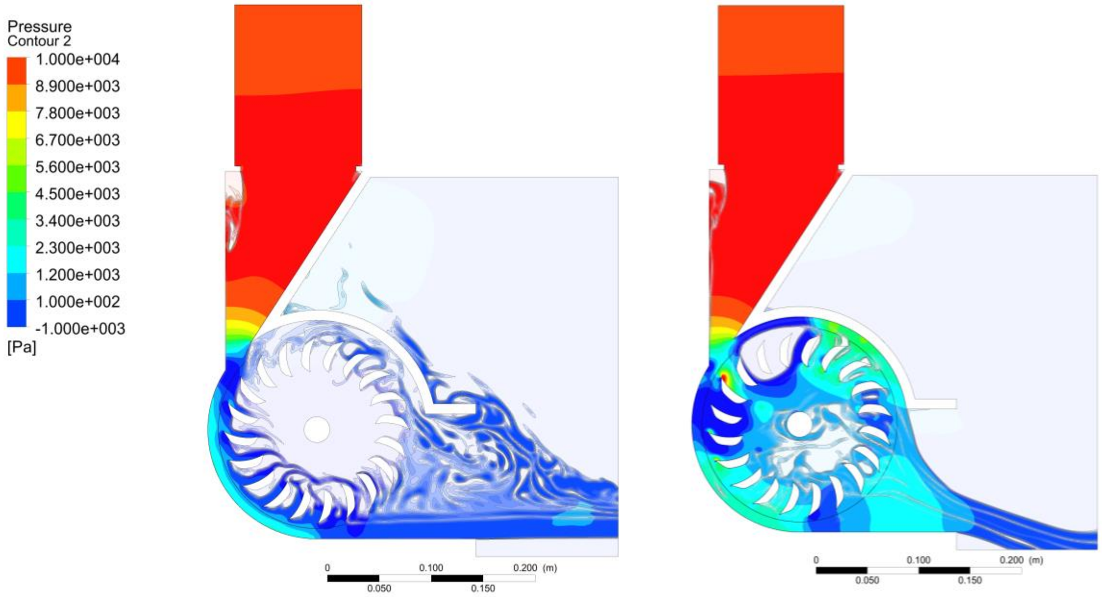

a) Preload 0 N.m b) Preload 45 N.m

Fig. 4. Pressure contour on different preload acting on its blade

Streamline is used to study the process of converting energy from water to blades (see Figure 5). In Figure 5(a), on preload 0 N.m, streamline contour shows only a small portion of water mashing the blade. Also seen, in preload 0 N.m, the conversion energy process on the second stage di not nearly occur. Whereas when the preload is given, the turbine rotation is not so fast that it can be seen when the preload is given at 30 N.m, the water that hit the blade is increasing and so on. It can be concluded that when the turbine does not have preload, the energy conversion process in the second stage is almost no (so that performance is not optimum) due to the fast turning wheel so that the water cannot hit the blade.

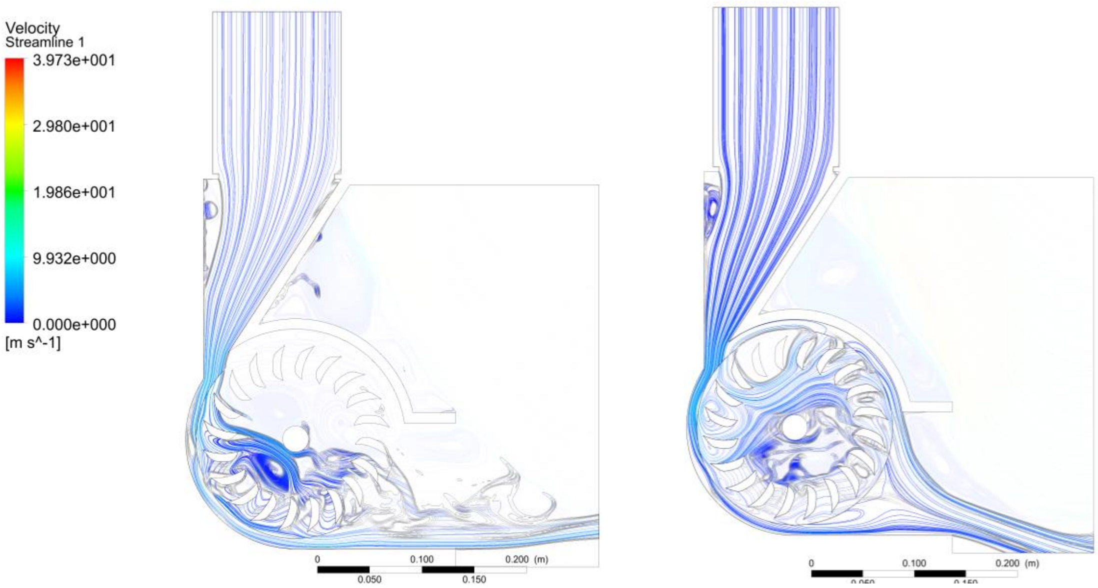

a) Preload 0 N.m b) Preload 45 N.m

Fig. 5. Streamline on different preload acting on its blade

Figure 6(a) is a pressure contour from the Sammartano [17] simulation result and Figure 6(b) is a pressure contour from this simulation result. From the two figures above, it can be seen that both show similar pressure patterns. The pressure is initially high then starts to decline slowly before finally, the pressure will rise again when the water hits the blade for the first time. The same phenomena also can be seen in the impeller area, which has the least pressure value.

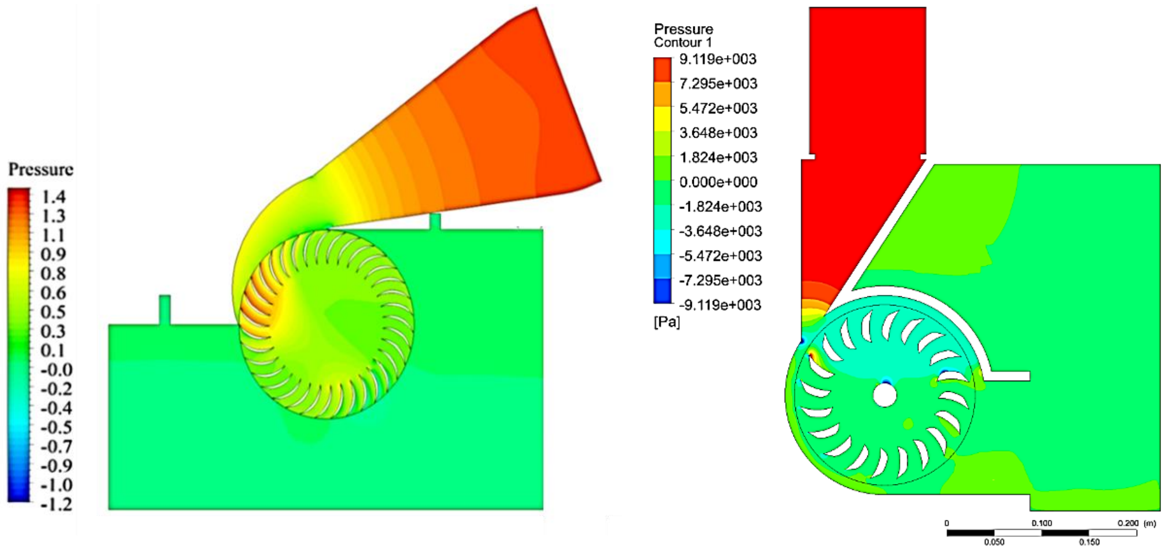

a) Sammartano's Pressure contour [17] b) Pressure contour Preload 30 N.m

Fig. 6. Pressure contour

Figure 7(a) is a pressure contour from the Zaffar [18] simulation result and Figure 7(b) is a streamline from this simulation result. From the two figures below, it can be seen that both show a similar pattern.

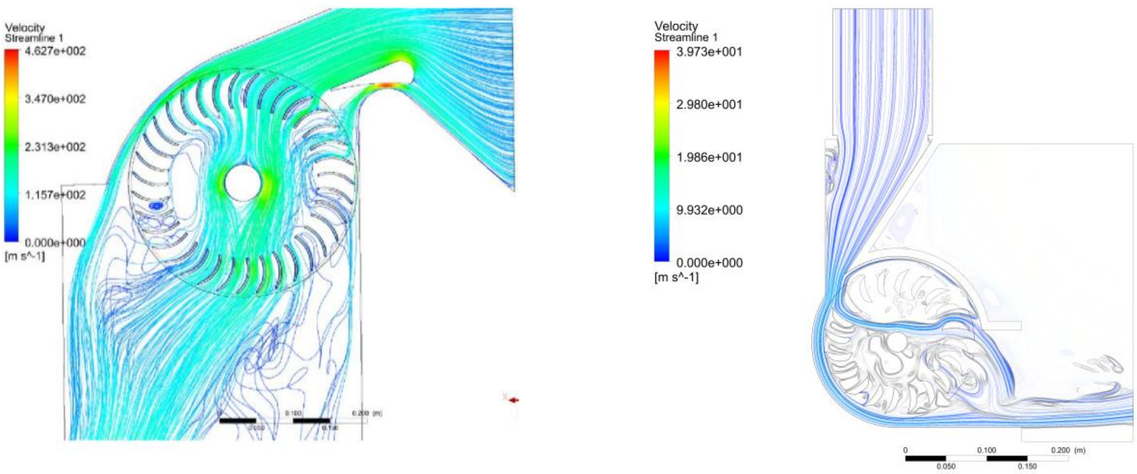

a) Zaffar's streamline [18] b) Streamline Preload 30 N.m

Fig. 7. Streamline

4. Conclusions

Computational results using the 6-DoF feature with preload variation obtain similar to testing. So this can be an alternative to predict the performance of a pico-hydro cross-flow turbine. The computational results showed that used 45 N.m preload has more stable and had higher efficiency than the other preload variation. The 45 N.m preload produced 60.07% efficiency with the head condition of 1 meter and mass flow of 10.5 kg/s which is the highest efficiency rather than the other variation. Therefore, the effect of preload on the computational result is that the preload will produce a lower rotating speed value and a higher torque value when the given preload value increases.

Acknowledgment
This work supported by the Directorate of Research and Service Community (DRPM) Universitas Indonesia with grant No: 0050/UN2.R3.1/HKP.05.00/2019.

References

[1] International Energy Database, Energy Access Database, (2019).
[2] Kaygusuz, Kamil. "Renewable energy: Power for a sustainable future." *Energy exploration & exploitation* 19, no. 6 (2001): 603-626.
[3] Paish, Oliver. "Small hydro power: technology and current status." *Renewable and sustainable energy reviews* 6, no. 6 (2002): 537-556.
[4] Pokhrel, Sajjan. "Computational Modeling of A Williams Cross Flow Turbine." PhD diss., Wright State University, 2017.
[5] Adanta, Dendy, Richiditya Hindami, and Ahmad Indra Siswantara. "Blade Depth Investigation on Cross-flow Turbine by Numerical Method." In *2018 4th International Conference on Science and Technology (ICST)*, pp. 1-6. IEEE, 2018.
[6] S. Kumar Patro, T. kumar, A. kumar, S. sagar, K. kumar, and G. Satya Prasad. "Technical and Economic Feasibility of Pico Hydro Power Plants Integrated to Green Buildings." *Int. Res. J. Eng. Technol.* (2016): 2395.
[7] Montanari, R. "Criteria for the economic planning of a low power hydroelectric plant." *Renewable energy* 28, no. 13 (2003): 2129-2145.
[8] Adanta, Dendy, and Aji P. Prakoso. "The effect of bucketnumber on breastshot waterwheel performance." In *IOP Conference Series: Earth and Environmental Science*, vol. 105, no. 1, p. 012031. IOP Publishing, 2018.
[9] Li, Jinbo, Wenjing Du, and Lin Cheng. "Numerical simulation and experiment of gas-solid two phase flow and ash deposition on a novel heat transfer surface." *Applied Thermal Engineering* 113 (2017): 1033-1046.
[10] Zhao, Ge, Wei Li, and Jinsong Zhu. "A Numerical Investigation of the Influence of Geometric Parameters on the Performance of a Multi-Channel Confluent Water Supply." *Energies* 12, no. 22 (2019): 4354.
[11] Frank, Th, C. Lifante, H-M. Prasser, and F. Menter. "Simulation of turbulent and thermal mixing in T-junctions using URANS and scale-resolving turbulence models in ANSYS CFX." *Nuclear Engineering and Design* 240, no. 9 (2010): 2313-2328.
[12] Adanta, Dendy, Warjito Budiarso, Ahmad Indra Siswantara, and Aji Putro Prakoso. "Performance comparison of NACA 6509 and 6712 on pico hydro type cross-flow turbine by numerical method." *Journal of Advanced Research in Fluid Mechanics and Thermal Sciences* 45, no. 1 (2018): 116-127.
[13] Fluent, A. N. S. Y. S. "Ansys fluent theory guide." *ANSYS Inc., USA* 15317 (2011): 724-746.
[14] G. Engineering. "Research and Development on Critical (Sonic) Flow of Multiphase Fluids through Wellbores in Support of Worst-Case-Discharge Analysis for Offshore Wells." 2018.
[15] Phillips, Tyrone S., and Christopher J. Roy. "Richardson extrapolation-based discretization uncertainty estimation for computational fluid dynamics." *Journal of Fluids Engineering* 136, no. 12 (2014): 121401.
[16] Harinaldi, Budiarso. "Sistem Fluida Prinsip Dasar dan penerapan Mesin Fluida, Sistem Hidrolik, dan Sistem Penumatik." (2015).
[17] Sammartano, Vincenzo, Costanza Aricò, Armando Carravetta, Oreste Fecarotta, and Tullio Tucciarelli. "Banki-Michell optimal design by computational fluid dynamics testing and hydrodynamic analysis." *Energies* 6, no. 5 (2013): 2362-2385.
[18] Zaffar, Assad, Bilal Ibrahim, M. Awais Sarwar, Javed Ahmed Chattha, and Muhammad Asif. "Optimisation of blade profiles of cross flow turbine." *International Journal of Power and Energy Conversion* 9, no. 4 (2018): 311-326.